Varestraint weldability testing of cast ATI® 718Plus™—a comparison to cast Alloy 718

Citation for the original published paper (version of record):
Singh, S., Andersson, J. (2019). Varestraint weldability testing of cast ATI® 718Plus™—a comparison to cast Alloy 718. Welding in the World, Le Soudage Dans Le Monde, 63(2): 389-399. http://dx.doi.org/10.1007/s40194-018-0626-2

Welding in the World (2019) 63:389–399
https://doi.org/10.1007/s40194-018-0626-2

RESEARCH PAPER

Varestraint weldability testing of cast ATI® 718Plus™—a comparison to cast Alloy 718

Sukhdeep Singh[1] · Joel Andersson[2]

Received: 5 April 2018 / Accepted: 5 July 2018 / Published online: 26 July 2018

Abstract
Varestraint testing of the newly developed cast ATI® 718Plus™ after pseudo-HIP (hot isostatic pressing) heat treatments showed that the extent of solidification cracking was independent of the heat treatment condition. The susceptibility towards heat-affected zone (HAZ) liquation cracking was found to be related to the heat treatment dwell time rather than the temperature. The heat treatments at 1120 and 1190 °C for 24 h were the most susceptible to cracking. On the other hand, heat treatments at 1120, 1160 and 1190 °C for 4-h dwell time exhibited the least amount of cracking. The solidification cracking was found to be similar whereas the HAZ liquation cracking was lower for ATI® 718Plus™ after the heat treatment at 1120 and 1190 °C for 4-h dwell time in comparison to cast Alloy 718.

Keywords Hot cracking · Cast ATI® 718Plus™ · Cast alloy 718 · Varestraint testing · Backfilling

1 Introduction

ATI® 718Plus™ has been developed in response to the demand for an alloy that could surpass the operating temperature limit of Alloy 718 while maintaining good fabricability, which has been one of the success factors of Alloy 718 compared to other concurrent superalloys used for high-temperature applications. The newly developed ATI® 718Plus™, which is strengthened primarily by the γ' phase, has an advantage of ~ 50 °C in terms of maximum operating temperature to the γ'' strengthened Alloy 718 [1, 2].

Recommended for publication by Commission IX - Behaviour of Metals Subjected to Welding

✉ Sukhdeep Singh
sukhdeep.singh@chalmers.se

Joel Andersson
joel.andersson@hv.se

[1] Department of Industrial and Materials Science, Chalmers University of Technology, SE-41296 Gothenburg, Sweden

[2] Department of Engineering Science, University West, SE-46181 Trollhättan, Sweden

The similarity in the solidification range of ATI® 718Plus™ to that of Alloy 718 [2, 3] makes it very promising for being developed for cast structures. A special composition has been under research with regard to increased amount of Nb for the cast version of ATI® 718Plus™ [4]. Cast components usually require homogenisation heat treatments prior to any manufacturing process, e.g. welding. From the industrial perspective, it is of interest to use similar heat treatment guidelines for ATI® 718Plus™ as for cast Alloy 718. Hot isostatic pressing (HIP) heat treatments for cast alloys such as Alloy 718 have been developed to avoid incipient melting of the Laves eutectic constituent, at soak temperatures and dwell times of 1120 °C/4 h [5] and 1190 °C/4 h [6, 7]. In a previous research study, Singh et al. [8] investigated the hot cracking susceptibility of cast Alloy 718 by Varestraint testing after HIP at the above-mentioned temperatures. It was found that although similar response in solidification cracking of the two conditions, the heat-affected zone (HAZ) liquation cracking susceptibility was higher for the heat treatment of 1190 °C (HIP 1190 °C/4 h + 870 °C/10 h and furnace cooling to 650 °C/1 h in vacuum + 950 °C/1 h + air cooling) [5], than the 1120 °C (HIP 1120 °C/4 h + 1050 °C/1 h and furnace cooling to 650 °C/1 h in vacuum +950 °C/1 h + air cooling) [6, 7].

Table 1 Composition of wrought ATI® 718 Plus™, cast ATI® 718 Plus™ and cast Alloy 718

Element (wt%)	Wrought ATI® 718Plus™	Cast ATI® 718Plus™	Cast Alloy 718
Ni	Bal.	Bal.	52.98
Cr	18	20.5	18.11
Fe	10	9.7	Bal.
Co	9	8.3	0.07
Nb	5.45	6.3	5.31
Mo	2.8	2.7	2.98
Al	1.45	1.5	0.42
Ti	0.7	0.8	0.99
C	0.02	0.05	0.05
W	1	1	0.01
Mn	–	0.01	0.03
Cu	–	0.1	0.01
Si	–	0.03	0.07
P	0.007	0.008	0.009
B	0.004	0.005	0.03

In the present study, the hot cracking susceptibility by Varestraint testing of cast ATI® 718Plus™ is evaluated after pseudo-HIP in regular laboratory without the effect of pressure at temperatures of 1120, 1160 and 1190 °C at 4-h dwell time, which are temperatures, below, at and above the incipient melting temperature of the Laves-γ eutectic, respectively [9]. In addition, the influence of two long dwell time heat treatments for 24 h at 1120 and 1190 °C, respectively, is evaluated in reference to the as-cast condition.

2 Experimental

The composition in weight percent of cast ATI® 718Plus™ is presented in Table 1. Differential scanning calorimetry (DSC) was performed by a Netzsch-STA 409 PC Luxx simultaneous DSC-TG equipment using heating and cooling rates of 20 °C/min for solidification sequences and comparison was made by simulation results obtained by JMatPro v8. The selected pseudo-HIP treatments were 1120, 1160 and 1190 °C for 4-h and 1120 and 1190 °C for 24-h dwell time followed by water quenching in order to avoid any precipitation of γ′. These five conditions were tested in reference to the as-cast condition.

Three test plates for each condition were tested using longitudinal Varestraint weldability testing at augmented strain levels of 1.1, 1.6, 2.1 and 2.7%. The test setup, available in reference [10], and welding conditions are the same as for the previous study of cast Alloy 718 [8]. The welding parameters are summarised in Table 2.

After testing, the plate surfaces were manually polished by fine abrasive paper to remove any oxide layer. Cracks were measured by a stereo microscope at × 57 magnification. Volume fraction of secondary precipitates was carried out by manual point count according to ASTM E562 [11]. Grain size measurements were conducted on two samples from each test plate (totally 144 samples). Macroetching was conducted by using the etching solution of HCL with mean concentration of 90%, 10% HNO_3, 120 g/l $FeCl_3$ powder heated to about 50 °C. Varestraint-tested samples as well as samples for determining the grain size were etched electrolytically by oxalic acid at 5 V and varying times and characterised by optical as well as scanning electron microscopy (LEO 1550 FEG-SEM with Oxford electron dispersive X-ray spectroscopy).

Table 2 Parameters used for Varestraint weldability testing using gas tungsten arc welding. Ar gas purity of 99.99%

Welding speed (mm/s)	Stroke rate (mm/s)	Welding current (A)	Arc length (mm)	Ar gas flow (l/min)
1	10	70	2	15

3 Results

3.1 Base metal microstructure

The base metal microstructure evolution after the pseudo-HIP treatments is shown in Fig. 1. The Laves phase constituent in

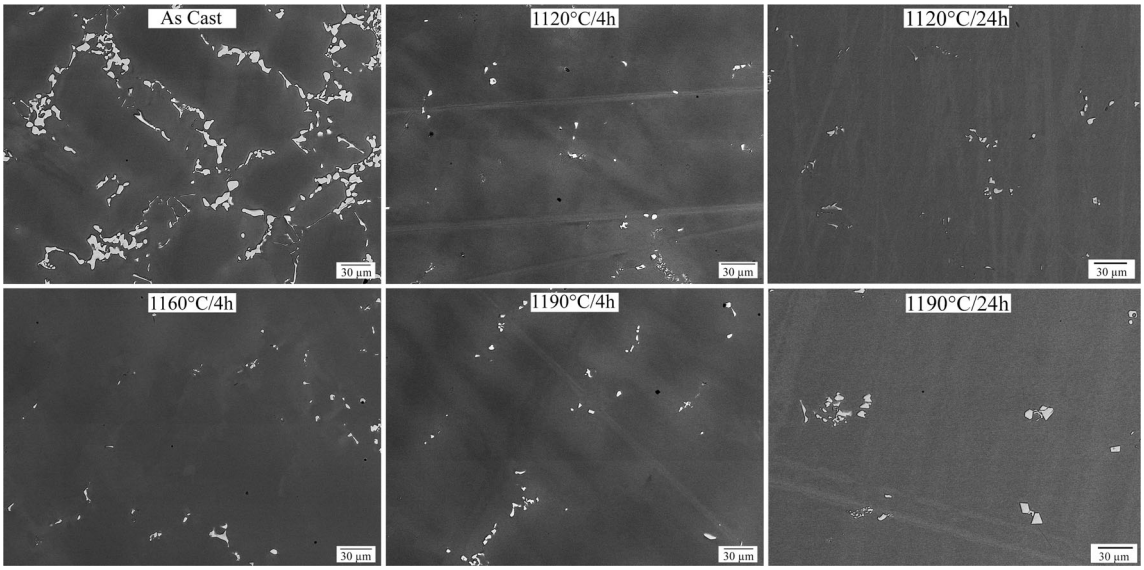

Fig. 1 Base metal microstructure map in the different conditions of cast ATI® 718Plus™

terms of volume fraction is presented in Table 3. The volume fraction of the Laves phase decreased from about 4.1% in the as-cast condition to about 0.3% after pseudo-HIP at 1120 °C/4 h and reached minimum values at the higher temperatures and longer dwell times. The same table also reveals the macrohardness and grain size values in each condition. The hardness dropped from 375 HV in the as-cast condition to 170–180 HV in the pseudo-HIP-treated conditions. Average grain size values remained similar of about 2.3 mm in all conditions except for 1190 °C/4 h, which exhibited a lower value of 1.7 mm.

3.2 Weld zone

Fusion zone (FZ) average total crack length (avg. TCL) against the augmented strain is presented in Fig. 2. It can be seen that, except for one data point with large standard deviation, there is no distinction in between the different conditions.

Weld bead dimensions were taken from four test plates for each condition and are summarised in Table 4. These values were measured from cross sections taken from the test plates experiencing maximum amount of bending.

Figure 3 shows an example of the variation in weld bead dimensions and weld grain structure in different cross sections taken from just one specific plate from the as-cast condition.

Figure 4 shows a typical solidification crack surrounded by an eutectic structure.

3.3 Heat-affected zone

Figure 5 shows the HAZ liquation cracking behaviour. The as-cast condition exhibited higher cracking response in respect to the heat treatments at short dwell times of 4 h. The latter, 1120 °C/4 h, 1160 °C/4 h and 1190 °C/4 h conditions, showed similar cracking susceptibility; however, the avg. TCL for the two conditions of 1120 °C/24 h and 1190 °C/24 h were higher despite the large standard deviation values. This is also confirmed by the higher total crack number values disclosed in

Table 3 Volume fraction of Laves, base metal hardness and grain size values for the different conditions

	As cast	1120 °C/4 h	1120 °C/24 h	1160 °C/4 h	1190 °C/4 h	1190 °C/24 h
Vv (%)	4.1 ± 0.7	0.3 ± 0.2	0.1 ± 0.1	0.1 ± 0.1	0.0 ± 0.0	0.0 ± 0.0
HV	375 ± 15	170 ± 0	180 ± 0	170 ± 5	170 ± 0	180 ± 5
GS (mm)	2.3 ± 0.5	2.2 ± 0.5	2.4 ± 0.5	2.3 ± 0.4	1.7 ± 0.4	2.5 ± 0.6

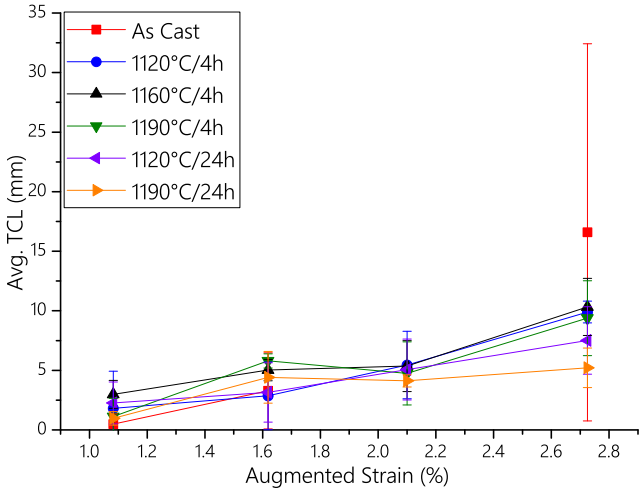

Fig. 2 Avg. TCL together with standard deviation values for FZ cracking

Table 4 Weld bead dimensions

Condition	Depth (mm)	Width (mm)	Depth/width
As cast	3.93 ± 0.24	8.2 ± 0.23	0.50 ± 0.03
1120 °C/4 h	4.3 ± 0.14	7.1 ± 0.14	0.61 ± 0.03
1160 °C/4 h	4.2 ± 0.16	7.35 ± 0.13	0.57 ± 0.02
1190 °C/4 h	4.23 ± 0.10	7 ± 0.14	0.60 ± 0.03
1120 °C/24 h	3.55 ± 0.19	7.84 ± 0	0.45 ± 0.02
1190 °C/24 h	3.68 ± 0.20	7.97 ± 0.10	0.46 ± 0.03

Table 5, where the total number of cracks were counted and averaged over the number of test plates.

Cracking in the as-cast condition propagated along interdendritic areas in the HAZ. In the heat-treated conditions, cracking followed the grain boundaries and was often connected to the FZ. The latter had clear signs of backfilling from the weld pool. An example of a partially backfilled crack is shown in Fig. 6.

4 Discussion

4.1 Cast ATI® 718Plus™

Figure 3 disclosed how the weld bead dimensions and weld grain structure changed within the same test plate. Also, Table 4 revealed the difficulty in obtaining similar weld bead dimensions between the different test plates. The difference in weld grain structure and weld bead dimensions is known to influence the weld cracking [12, 13]. However, despite these differences, solidification cracking was independent from the pre-weld heat treatment.

The relatively high scatter in the HAZ liquation cracking response is typical for castings and has previously been reported for cast Alloy 718 [8]. Cracking in the as-cast condition occurred interdendritically and was associated to liquation of the Laves phase (Fig. 7). Hardness values of 375 HV in the as-

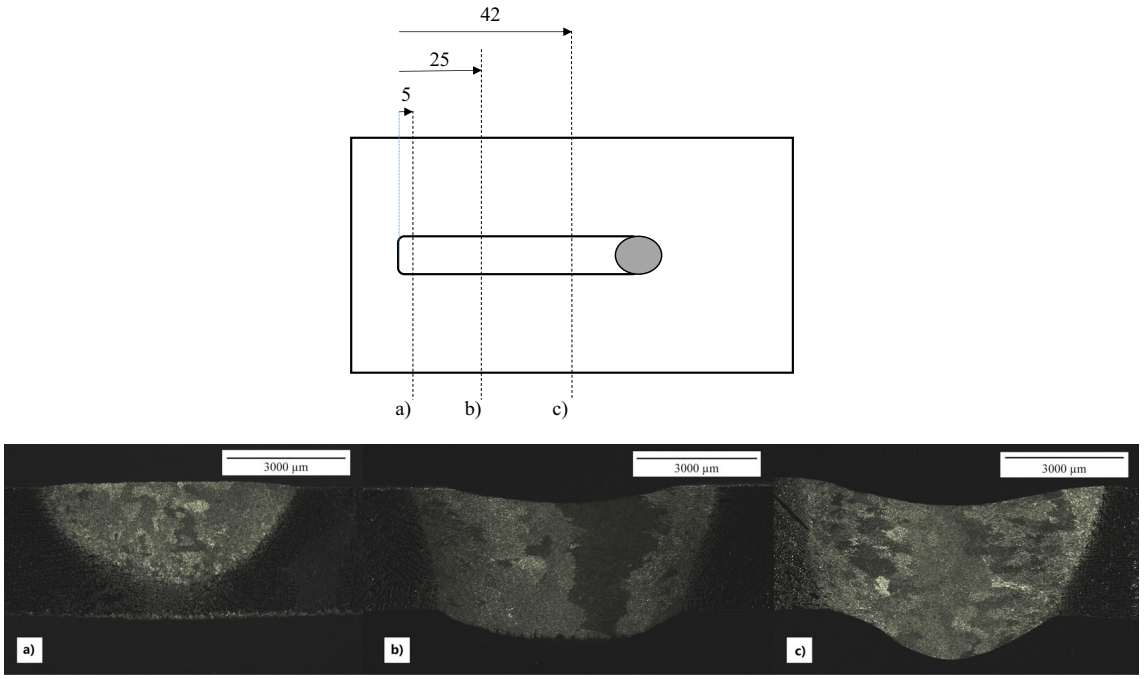

Fig. 3 Weld cross sections showing difference in weld grain structure and weld bead dimensions. The three cross sections are taken from the same test plate but at different locations, a) start of the weld, b) at steady-state condition and c) at area experiencing maximum amount of bending

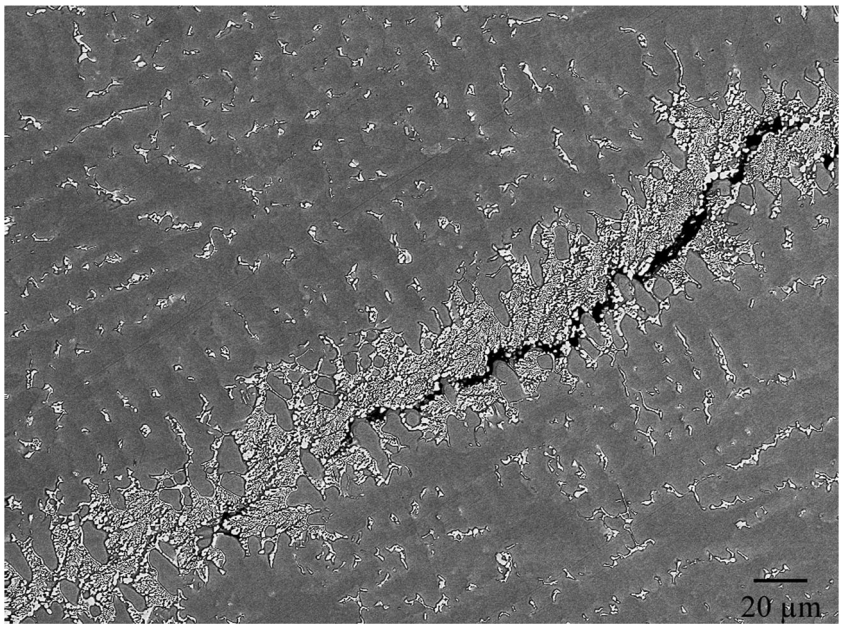

Fig. 4 A crack in the FZ surrounded by a solidified eutectic structure

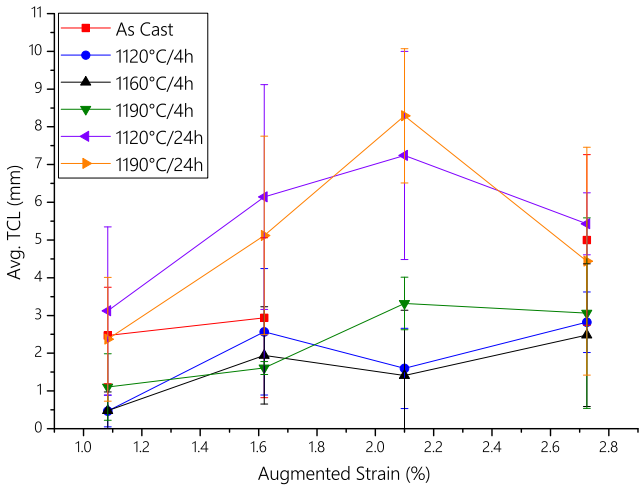

Fig. 5 Avg. TCL with standard deviation values for HAZ liquation cracking

cast condition are similar to that of the aged condition [9]. After the pseudo-HIP heat treatments, the Laves phase significantly reduced; however, in contrary to what is usually expected, grain growth did not occur. The relatively low hardness of 170 HV suggests that the γ′ phase precipitation was avoided by water quenching and a softer base metal was obtained which in turn also resulted in lower cracking for the 4-h dwell time heat treatments. The 24-h dwell time heat treatments, despite having similar values in grain size, hardness and higher degree of homogenisation, were the most susceptible to cracking. Similarly, Andersson et al. [9] found that the condition with the highest degree of homogenisation also exhibited the most amount of cracking when evaluating the effect of homogenisation treatments on the repair weldability of cast ATI® 718Plus™. It was hypothesised that grain boundary embrittlement can occur due the change in grain boundary wetting behaviour by redistribution of Nb. There are other variables which add to the complexity in reasoning of the results and are further discussed below.

In the results, it was pointed out that there was a lower grain size for the condition of 1190 °C/4 h (~ 1.7 mm) in comparison to the average of 2.3 mm for the other conditions. The grain size analyses were conducted on each side of the weld plates. The value for each condition in Table 3 is therefore the average values out of 24 samples. Figure 8 shows the grain structure in the as-cast plate, left side to the weld having average grain size of about 3.2 mm and right side with about 1.3 mm. The difference in grain size can be a result from the casting process, with the smaller grain size being closer to the mould walls and larger grains in the core. This could explain the lower grain size for the 1190 °C/4 h condition, having the test plates obtained from the side close to the mould wall.

Table 5 Total crack number averaged by the number of test plates

	As cast	1120 °C/ 4 h	1160 °C/ 4 h	1190 °C/ 4 h	1120 °C/ 24 h	1190 °C/ 24 h
TCN/samples	7.1	4	3.7	5.1	14	13.3

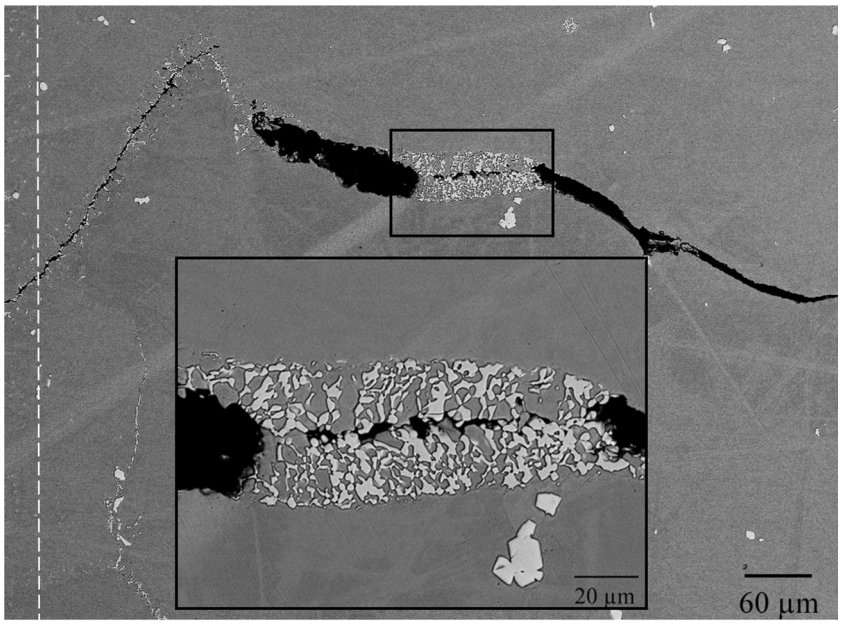

Fig. 6 A partially backfilled crack in the 1190 °C/24 h condition. The FZ line is marked by the dotted line

Grain size is often considered as an important parameter when assessing the cracking susceptibility. Smaller grain size is preferable over large grain size, especially in cast materials where grain size values can reach several millimetres [8, 14]. Previous studies on wrought and cast materials [15–17] covering the effect of grain size on weldability had relatively homogeneous grain size throughout the base metal. However, none of these studies have covered the weldability behaviour in relation to the varying grain size at the two sides of the weldment and especially with regard to how the strains would partition between large and small grains within the same test plate. The weld cross section showing the details of the cracks in Fig. 7 is obtained from the same test plate as in Fig. 8. Cracking was measured to the left side (large grain

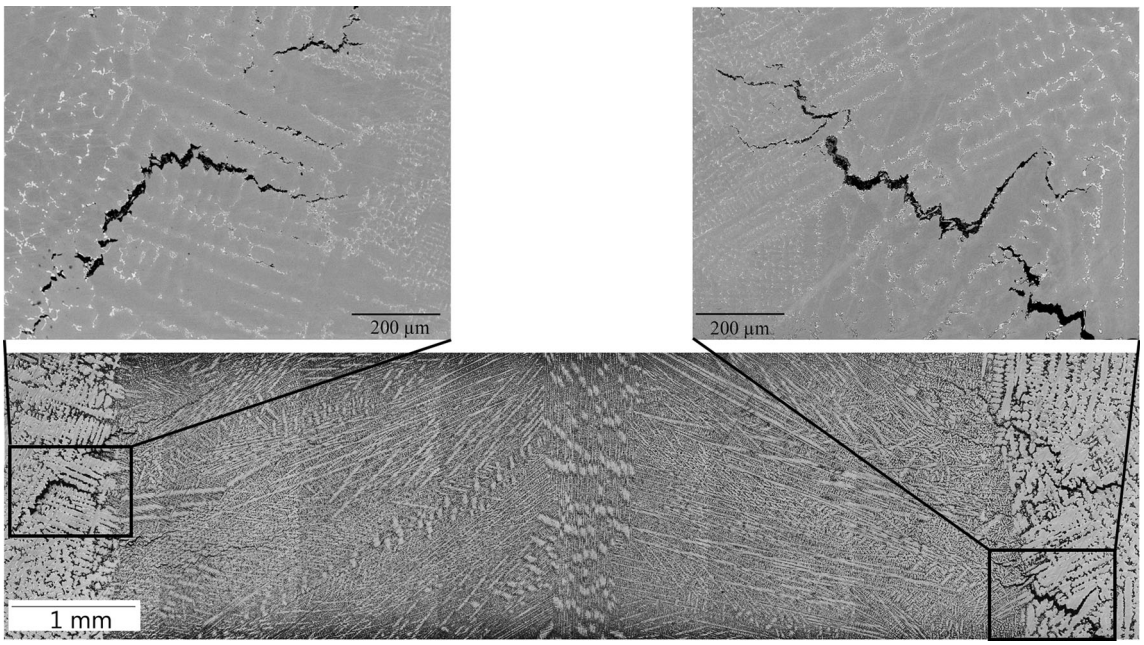

Fig. 7 Weld macro cross section of an as-cast test plate showing cracks in the interdendritic areas of the HAZ

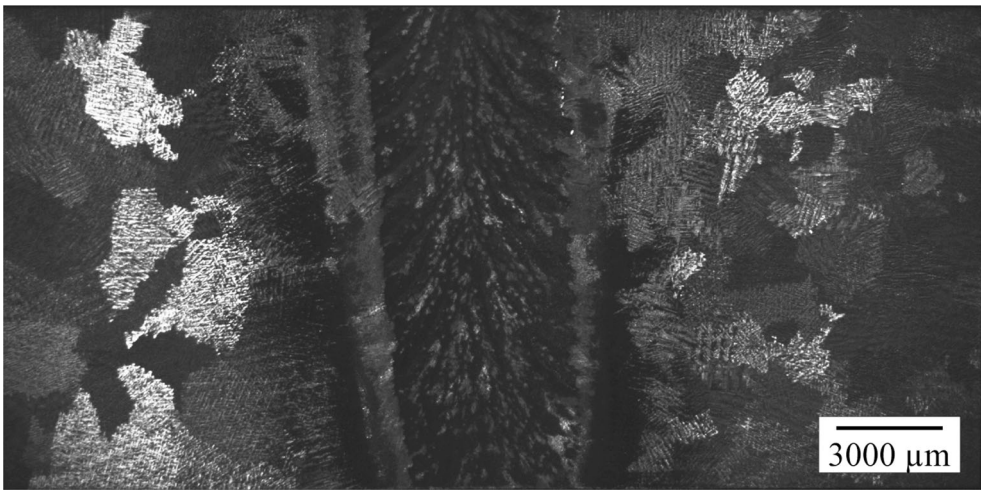

Fig. 8 Grain structure of an as-cast test plate

Table 6 Crack length and grain size values for the as-cast test plate in Figs. 7 and 8

	Left	Right
Avg. TCL (mm)	0.46 ± 0.14	0.40 ± 0.17
Grain size (mm)	3.2 ± 0.9	1.3 ± 0.1

size) and right side (small grain size) of the weldment but no difference was seen as disclosed in Table 6.

Figure 9 shows the grain structure in another test plate, exposed to 1190 °C/24 h heat treatment and Varestraint tested at 2.7% augmented strain. It reveals coarse grains with what seems to be small subgrains to the left side of weld, together with extremely small grains on the right-hand side suggesting that local recrystallisation had occurred (Fig. 10). This test plate exhibited an avg. TCL of length of 1.5 mm, at same

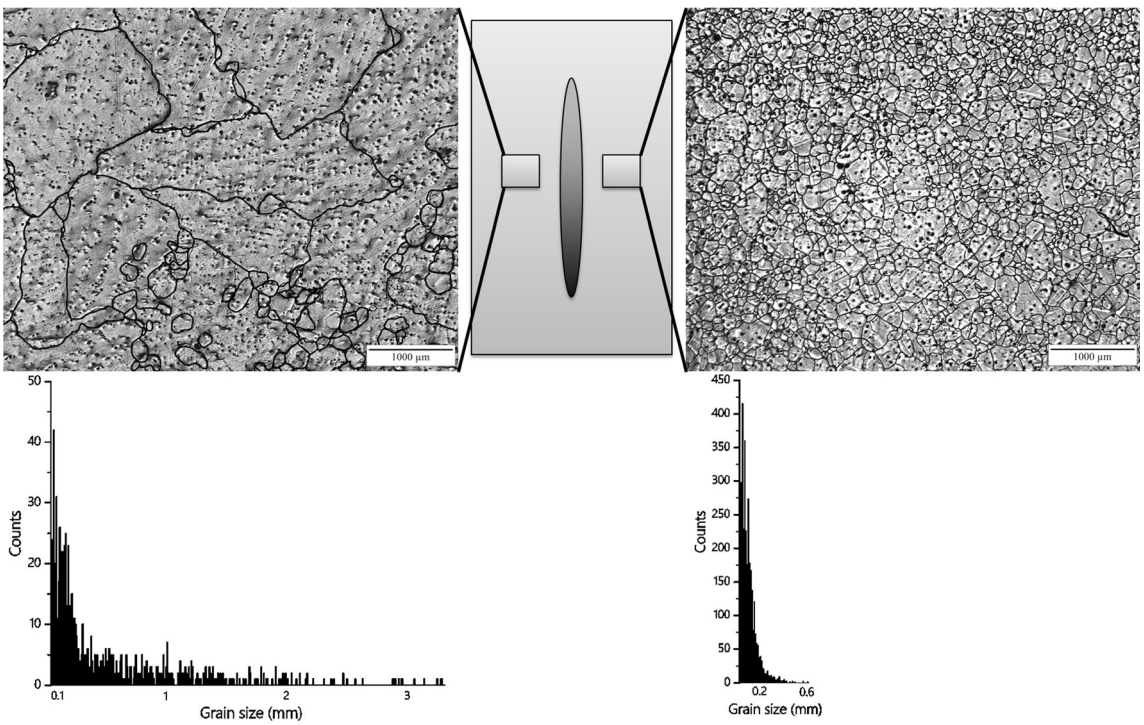

Fig. 9 Grain size distribution in a test plate subjected to heat treatment of 1190 °C/24 h and Varestraint tested at 2.7% augmented strain

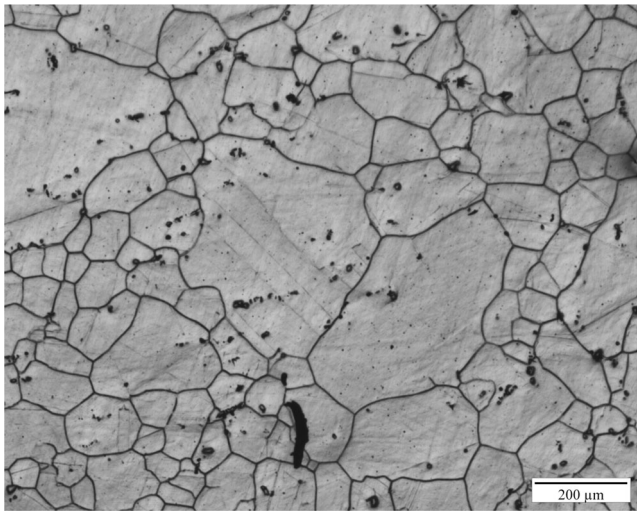

Fig. 10 Twin grains in the 1190 °C/24 h

Table 7 Extent of cracking in the test plate from Fig. 9

	Left	Right
Avg. TCL (mm)	0.67 ± 0.36	0.45 ± 0.26

order of magnitude as the 4-h dwell time heat treatments tested at 1.1% augmented strain.

Crack measurements on the two sides of the weld were conducted on a cross section extracted from the area experiencing maximum amount of bending. Measurements are summarised in Table 7.

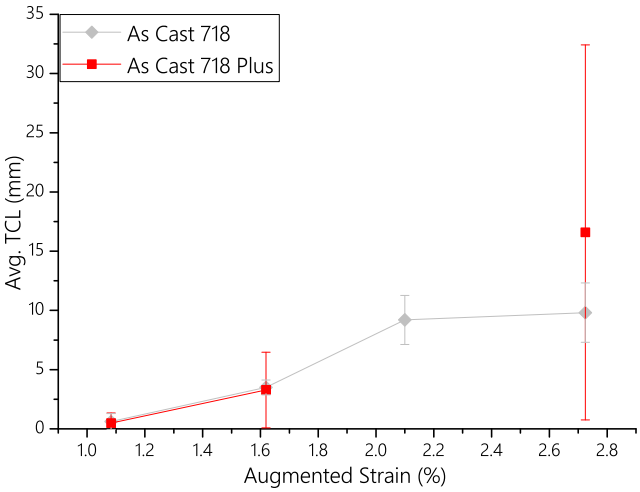

Fig. 11 Comparison of solidification cracking susceptibility for the two Ni- and Fe-Ni-based superalloys cast ATI® 718Plus™ and cast Alloy 718 [8]

Table 8 Solidification events for cast ATI® 718Plus™ and cast Alloy 718. Temperature values are in degree Celsius

	JMatPro			DSC		
	$T_{liquidus}$	$T_{solidus}$	Sol. range	$T_{liquidus}$	$T_{solidus}$	Sol. range
Cast ATI® 718Plus™	1328	1120	208	1328	1162	166
Cast Alloy 718	1357	1090	267	1334 [19]	1157 [19]	177 [19]

From the above considerations, it is difficult to judge whether the variation of the grain size within the test plate had any influence on cracking susceptibility as there is no previous theory explaining this behaviour or whether this can be related within the typical scatter for cast materials. The bi-modal grain size was found in a few test plates heat treated at 4-h dwell time as well but it was mainly found in the 24-h dwell time heat treatments. This behaviour is not well understood and more advanced characterisation is necessary to say whether this has an effect on weldability or not.

4.2 Comparison to cast Alloy 718

Solidification cracking susceptibility of the as-cast ATI® 718Plus™ is compared in reference to that of the cast Alloy 718 [8] in Fig. 11. However, no clear distinction is seen. This can be attributed to the similarity in solidification temperature range between the two alloys, with a difference of only about 11 °C (Table 8). Solidification cracking of an alloy is often considered to be influenced by the solidification range, where

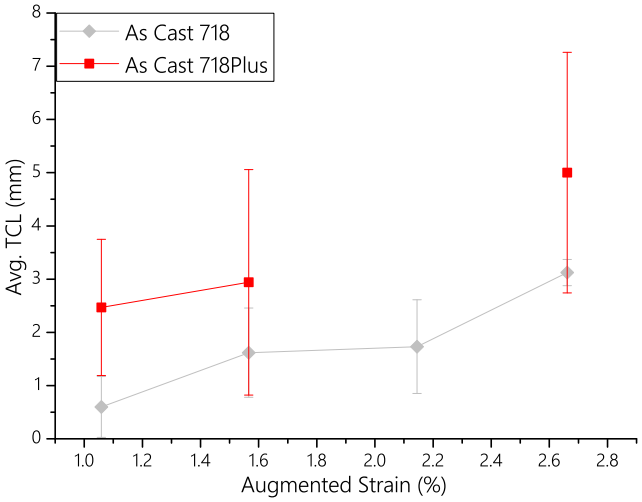

Fig. 12 Comparison in HAZ liquation cracking between as-cast ATI® 718 Plus™ and as-cast Alloy 718

Table 9 Comparison of volume fraction of secondary precipitates, base metal hardness and grain size values for the different conditions of cast ATI® 718Plus™ and cast Alloy 718

	Cast ATI® 718Plus™			Cast Alloy 718		
	As cast	1120 °C/ 4 h	1190 °C/ 4 h	As cast	HIP-1120	HIP-1190
Vv (%)	4.0 ± 0.5	0.3 ± 0.2	0.0 ± 0.0	3.7 ± 0.6*	1.7 ± 0.1*	1.3 ± 0*
HV	375 ± 15	170 ± 0	170 ± 0	260 ± 20	220 ± 30	210 ± 20
GS (mm)	2.3 ± 0.5	2.2 ± 0.5	1.7 ± 0.4	1.7 ± 0.1	2.6 ± 0.3	3.3 ± 0.3

*Volume fraction of Laves and NbC

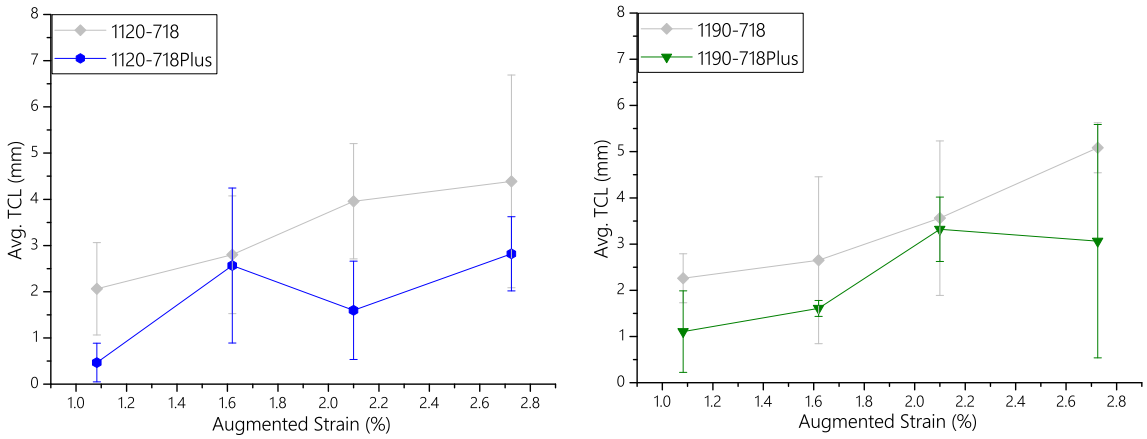

Fig. 13 Comparison in HAZ liquation cracking behaviour between cast ATI® 718Plus™ and cast Alloy 718 heat treated at 1120 °C/4 h and HIP-1120 in the left figure. On the right, comparison between cast ATI® 718Plus™ at 1190 °C/4 h and cast Alloy 718 at HIP-1190

a wider range promotes a more crack-susceptible alloy in comparison to small solidification temperature range [18].

Regarding HAZ liquation cracking, the as-cast ATI® 718Plus™ exhibited a higher cracking susceptibility than the as-cast Alloy 718 (Fig. 12). From Table 9, the volume fraction of secondary precipitates were similar, but the base metal hardness differed by about 100 HV.

Interestingly, after the heat treatments, the cracking susceptibility of cast ATI® 718Plus™ is lower than that of cast Alloy 718 (Fig. 13).

For cast Alloy 718, it was found that even though the segregation reduced with increasing pre-weld heat treatment temperature, the amount of cracking, however, increased with the increase in grain size. The difference in cracking susceptibility was

Table 10 Extent of backfilled cracks at 1.1 and 2.1% strain for cast ATI® 718Plus™ and cast Alloy 718

		Cast ATI® 718Plus™		Cast Alloy 718	
		1120 °C/ 4 h	1190 °C/ 4 h	HIP-1120	HIP-1190
2.1%	Avg. crack length	1.42 ± 0.61	1.36 ± 0.47	1.20 ± 0.54	0.92 ± 0.51
	Avg. backfilled length	0.59 ± 0.27	0.61 ± 0.31	0.48 ± 0.28	0.26 ± 0.11
	%	41	45	40	28
1.1%	Avg. crack length	1.55 ± 0.55	1.24 ± 0.50	0.82 ± 0.30	0.77 ± 0.25
	Avg. backfilled length	0.88 ± 0.53	0.66 ± 0.43	0.27 ± 0.22	0.36 ± 0.13
	%	57	53	33	47

% = (avg. crack length / avg. backfilled crack length) × 100

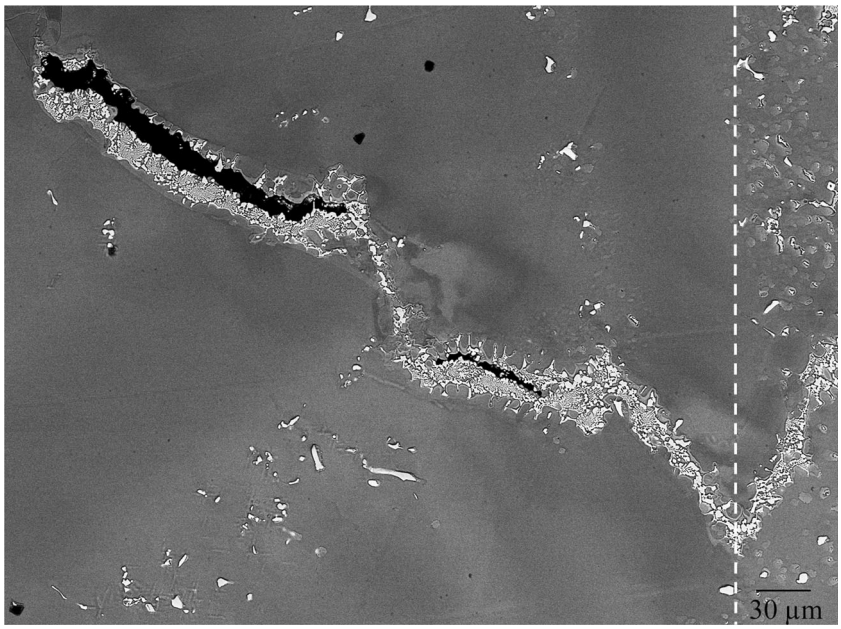

Fig. 14 Partial backfilling of a HAZ crack in cast Alloy 718. FZ line is indicated by the dotted line

clearly noticeable above the saturation level, at 3–4% augmented strain [8]. In this study, however, testing was done below the saturation point and no distinction in between the pre-weld heat treatments at 1120 °C/4 h and 1190 °C/4 h were seen.

Comparing the values in Table 9, it can be seen that the volume fraction of secondary precipitates and hardness values were higher for cast Alloy 718 in the heat-treated conditions but the average grain size was significantly larger only for the HIP-1190 condition. Therefore, the synergetic effect of volume fraction, hardness and grain size seem to be involved when evaluating the difference in cracking susceptibility.

The backfilling effect for the two alloys was also quantified for two selected strain levels of 1.1 and 2.1% in terms of avg. TCL and avg. backfilled length. However, no distinction was seen. The Varestraint test is believed to not be the best testing method when evaluating the effect of backfilling due to the applied augmented strain [20]. Data is provided for reference in Table 10. Example of partially backfilled crack for cast Alloy 718 is shown in Fig. 14.

5 Conclusions

5.1 Cast ATI® 718Plus™

- The solidification cracking was independent of the pre-weld condition.
- The as-cast condition was more crack susceptible in the HAZ than the heat treatments at 1120, 1160 and 1190 °C at 4-h dwell time but less than the 1120 and 1190 °C 24-h dwell time heat treatments.
- The only difference in the heat-treated conditions is between the short and long dwell time heat treatments, where 1120 and 1190 °C at 24 h showed more extensive HAZ liquation cracking than the 1120, 1160 and 1190 °C at 4 h.

5.2 Comparison of cast ATI® 718Plus™ to cast Alloy 718

- The solidification cracking of the two alloys were similar.
- The as-cast condition of the newly developed ATI® 718Plus™ exhibited higher amount of HAZ cracking than the as-cast condition of Alloy 718.
- After the heat treatments at 1120 and 1190 °C at 4 h, the HAZ liquation cracking in cast ATI® 718Plus™ decreased in reference to that of HIP Alloy 718.
- No difference in backfilling effect is seen.

Acknowledgements The authors want to acknowledge Ms. Tahira Raza, Mr. Kjell Hurtig and Mr. Sebastian Östlund for the help provided during testing and characterisation.

Funding information The study was funded by the Swedish Energy Agency and GKN Aerospace Sweden AB.

References

1. Cao WD, Kennedy R (2004) Role of chemistry in 718-type alloys—Allvac® 718Plus™ alloy development. Superalloys 2004: 91–99
2. Cao WD (2005) Solidification and solid state phase transformation of Allvac® 718Plus™ alloy, in Superalloys 718, 625 and various derivatives 2005, pp 166–177
3. Andersson J, Raza S, Eliasson A, Surreddi KB (2014) Solidification of Alloy 718, ATI 718Plus® and Waspaloy. In: 8th International Symposium on Superalloy 718 and Derivatives
4. Peterson B, Frias D, Brayshaw D, Helmink R, Oppenheimer S, Ott E, Benn R, Uchic M (2012) On the development of cast ATI 718Plus® Alloy for structural gas turbine engine components. In: Superalloys 2014 Conference. TMS
5. Barron ML (1999) Crack growth-based predictive methodology for the maintenance of the structural integrity of repaired and nonrepaired aging engine stationary components. GE Aircraft Engines Cincinnati OH
6. Snyder SM, Brown EE (1988) Laves free cast + hip nickel base superalloy US Patent No 4,750,944
7. Paulonis DF, Schirra JJ (2001) Alloy 718 at Pratt & Whitney—historical perspective and future challenges. Superalloys 718.625, 706:13–23
8. Singh S, Andersson J (2018) Hot cracking in cast alloy 718. Sci Technol Weld Join:1–7
9. Andersson J, Sjöberg G, Larsson J (2010) Investigation of homogenization and its influence on the repair welding of cast Allvac 718Plus (®). In: Proceedings of The 7th International Symposium on Superalloy 718 and Derivatives, TMS (The Minerals, Metals and Materials Society), pp 439–454
10. Andersson J, Jacobsson J, Lundin C (2016) A historical perspective on Varestraint testing and the importance of testing parameters. In: Cracking phenomena in welds IV. Springer International Publishing, pp 3–23
11. STANDARD, A. S. T. M (2008) Standard Test Method for determining volume fraction by systematic manual point count. ASTM E562–08
12. Kou S (2003) Solidification and liquation cracking issues in welding. JOM 55(6):37–42
13. Srinivasan G, Bhaduri AK, Shankar V, Raj B (2013) Evaluation of hot cracking susceptibility of some austenitic stainless steels and a nickel-base alloy. Weld World 52(7–8):4–17
14. Woo I, Nishimoto K, Tanaka K, Shirai M (Jan. 2000) Effect of grain size on heat affected zone cracking susceptibility. Study of weldability of Inconel 718 cast alloy (2nd Report). Weld Int 14(7):514–522
15. Thompson RG, Cassimus JJ, Mayo DE, Dobbs JR (1985) The relationship between grain size and microfissuring in alloy 718. Weld J 64(4):91–96
16. Hong JK, Park JH, Park NK, Eom IS, Kim MB, Kang CY (May 2008) Microstructures and mechanical properties of Inconel 718 welds by CO2 laser welding. J Mater Process Technol 201(1–3): 515–520
17. Huang X, Richards NL, Chaturvedi MC (Dec. 2004) Effect of grain size on the weldability of cast Alloy 718. Mater Manuf Process 19(2):285–311
18. Borland J (1960) Generalized theory of super-solidus cracking in welds (and castings). Br Weld J 7(8):508–512
19. Andersson J (2011) Weldability of precipitation hardening superalloys—influence of microstructure. Phd Thesis, Chalmers University of Technology
20. Lippold JC, Sowards JW, Murray GM, Alexandrov BT, Ramirez AJ (2008) Weld solidification cracking in solid-solution strengthened Ni-base filler metals. In: Hot cracking phenomena in welds II, pp 147–170